Kurdistan Journal of Applied Research (KJAR)
Print-ISSN: 2411-7684 | Electronic-ISSN: 2411-7706

Website: Kjar.spu.edu.iq | Email: kjar@spu.edu.iq

# The Impact of Non-constant Inertia and Nonlinear Damping on the Torsional Vibration Characteristics of Internal Combustion Engine Including External Forces

**Hameed D. Lafta**
Mechanical Engineering Department
Technical College of Engineering
Sulaimani Polytechnic University
Sulaimani, Iraq
Hameed.lafta@spu.edu.iq

**Article Info**

***Volume 7 - Issue 2- December 2022***

***DOI: 10.24017/Science.2022.2.3***

***Article history:***

Received: 27/08/2022
Accepted: 07/10/2022

***Keywords:***

Internal combustion engines, Nonlinear torsional vibration, Variable inertia, nonlinear damping, excitation torques.

**ABSTRACT**

***A nonlinear torsional vibration is an essential problem arises in internal combustion engine due to cyclic variation in inertia and gas pressure forces. A linear or lumped model of engine effective inertia reveals obvious simulation errors. An accurate and sophisticated nonlinear dynamic detailed model overcomes the obvious simulation errors of the linearized models. The present work studies the effect of the non-conservative forces and nonlinear damping on the torsional vibration of single-cylinder internal combustion engines. Comprehensive dynamic modeling based on a developed expression for the instantaneous kinetic energy of the reciprocating parts and a general model of the overall kinetic energy of the system in terms of the inertia parameters were derived. The nonlinear dynamic equations are derived using the Lagrange's equation considering the nonlinear parameters of the variable inertia of reciprocating parts and the nonlinear internal damping factors of the crank assembly. The damped-forced response of a slider-crank assembly of the engine considering the non constant inertia is investigated using the numerical integration technique. The results of the nonlinear torsional vibration analysis show that the cyclic variation in engine effective inertia and natural frequency arise due inertia effect activate the phenomenon of secondary rolling excitation torque. As well as, the amplitude of the external excitation torque is strengthened by the secondary excitation inertia torque and introduces multi resonance amplitudes phenomenon and widening the critical range of engine speed which results in producing of dangerous vibrational stress amplitudes. Also, the damped forced results indicate that the presents of damping lead***

***to a vital reduction in the amplitude of torsional displacement and excitation torques. The present work attempts to enhance the knowledge of the nonlinear linear torsional vibration analysis for the reciprocating engine crankshaft assembly.***

## 1. INTRODUCTION

Nonlinear characteristics of torsional vibration in internal combustion engines (ICE)are important phenomena that occurs due to excitation forces, cyclic variations resulting from the pressure of the ignited gases, and changes in inertia loads produced by engine reciprocating parts through the conversion of rotary motion into the linear one [1]. By assuming that the dynamical parameters are to be constant, represent the main source of the errors in theoretical dynamic modeling of the crankshaft assembly and more sophisticated models are often required [2].Due to the torsional vibrations in ICE there is a danger for this engine in that the cyclic variation in the speed of the reciprocating parts and their associated inertia give a rise for appearing of a range of resonance frequencies in the normal range of operating rotational speed of the engine which produces amplitudes of torsional vibrations of crankshaft may exceed acceptable values [3]. Also, material nonlinearity, nonlinear friction, and nonlinear viscous friction result in nonlinear stiffness and damping [4].Normally, linearization of nonlinear dynamic parameters in practical modeling can definitely leads to induce an inaccurate modeling; thus, finding of non-linear dynamical parameters with accurate expressions is vital and important in developing more adequate equations describing the nonlinear torsional vibration of the internal combustion engines [5, 6].

The literatures in the subsequent sections summarize the effect of variable inertia-reciprocating masses, the nonlinear damping, and the gas force variation on the nonlinear torsional vibration analysis of ICE. For instance, Ying et al. [7] developed variable inertia model to study the nonlinear dynamic characteristics of a crankshaft assembly in an internal combustion engine. Their study is carried on equivalence method of the instantaneous kinetic energy. The dynamic equations are derived by using the Lagrange rule taking into account the nonlinear parameters. The Eigenvector method is used to determine the system natural frequencies and mode shapes, and the forced vibration response is investigated by using the numerical integration technique. Based on the system matrix method, the simulation results are compared with the detailed and lumped mass models. The results explain that the secondary excitation torque generated by the variable inertia excites the $2^{nd}$order rolling vibration. Also the additional damping torque due to the variation in inertia represents the main nonlinear factor, and the increase in the torsional displacement of the system caused by the high-order secondary excitation torque. N. K. Joshi and V. K. Pravin [8] analyzed the effect of constant and non constant inertia on the torsional vibration of the engine of marine. Their analysis involves modal, order, harmonic, and stress analyses correspondent to the engine critical speeds. They concluded that when the variable inertia factor is considered, the range of the critical speed was widened and the system may undergo severe vibration stress amplitudes. In analyzing the torsional vibrations of reciprocating machines, identification, modeling, and a better understanding of the damping characteristics are of particular importance and complexity, and, this complexity has led to the analysis of machines either without damping or simple damping with approximations of actual state [4, 9].Y. Wang and T. C. Lim [4] developed a comprehensive expression for the damping of reciprocating engines experimentally. Their study decomposed the internal damping in reciprocating engines into viscous friction, material, and non-friction (including impactive) types. The experimental results indicate that the non-friction damping contribution is very significant and most of them come from the revolute joints at both ends of the connecting rod. This study also shows that the measured damping levels in the reciprocating engine are sensitive to clearance in the joints of the connecting rod, and are insensitive to the types of lubricating oil and material used. M. S. Pasricha [10] presented the equation of motion based on a lumped model of reciprocating

masses with considering the variation in the inertia of the system with key non dimensional parameters to include both damping and external excitations to predict the complete response of an equivalent single-cylinder engine system. The results show a secondary resonance effect arising from the variable inertia characteristics of the system, and under certain circumstances, it can have a serious impact on torsional vibration. Nenad Vulić et al. [11] studied the engine excitation and damping on the torsional vibration of ship propulsion system including moments of inertia of effective masses, shaft stiffness, the actual damping of the shaft components and the propulsion engine excitation moments and forces. They systematically compared different models of damping in order to enable designers to correctly selected damping model. An important outcome of their analyses showed that the continuous operation of the engine drive-propulsion at the range of speed of rotating shaft of approximately 60 rpm should be evaded (barred-shape speed zone) to minimize the conceivable damage of the system caused by the excitation at resonance conditions.Tao Li et al. [12] studied the impact of frictional damping between the engine cylinder and the slider piston on the nonlinear torsional vibration of a reciprocating compressor considering the variation in the inertia of the slider-crank mechanism under undamped and damped conditions. The results indicate that when considering the friction between sliding-rotating parts, the shafting system second order natural frequency show a "maximum-minimum-maximum" cyclictrend; also, with the increase in the friction coefficient, the shafting system amplitude and the maximum vibration speed show an upward trend. While with increases in engine speeds, the shaft system vibration altered from a non-periodic to the suggested periodic situation, however, the amplitude of vibration tend to be decreased in magnitude dramatically.

Based on the literature above the nonlinear dynamic parameters have a great effect on the nonlinear torsional vibration characteristics of slider-crank assembly and to develop a satisfied functional relationship between the variable inertia and the crank shaft angle is an improved and effective method. Thus, the present work aims to derive a dynamical relationship establishes the interaction between the secondary resonance effects and the harmonic excitations considering the variation in the inertia of the reciprocating parts under the effect of nonlinear damping and gas forces. A detailed model of the instantaneous kinetic energy of reciprocating parts is derived taking into account the variation in the inertia of the crank shaft assembly. A more general form of nonlinear torsional vibration equations set is derived in terms of inertia and damping parameters using the Lagrange's equation for free-damped and forced-damped models. The influence of non- constant inertia and nonlinear damping on the torsional vibration characteristics of the crankshaft-slider mechanism are investigated by applying the numerical integration technique. The simulation results are analyzed and discussed for free-damped and forced-damped models over a range of crank angle and frequency ratios to establish the influence of the nonlinear dynamic parameters.

## 2. MATHEMATICAL MODELLING

### *2.1. Derivation of Instantaneous Inertia Expression*

The kinematical representation of a single-cylinder internal combustion engine is shown in fig (1) below.

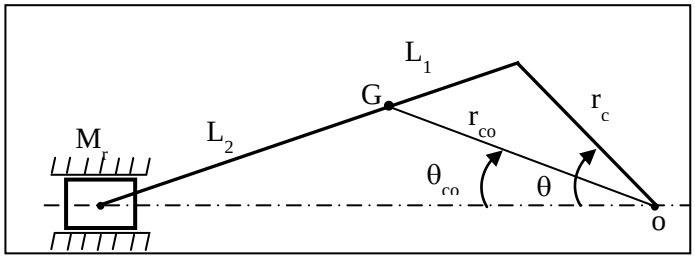


**Figure 1:** Kinematical representation of slider-crank reciprocating engine.

The developed expression of the connecting rod instantaneous kinetic energy is based on the definition of the instantaneous fiction radial distance that connect the center of mass of the connecting rod (G) to the center of rotation of the crankshaft (O), as shown in figure (1). Consequently, from the kinematical relationship of slider-crank mechanism, the expression of the radial distance ($r_{co}$) and its associated angular displacement ($\theta_{co}$) are given by:

$$r_{co}(\theta) = \sqrt{(L_1\lambda sin\theta)^2 + (L_2\sqrt{1-(\lambda sin\theta)^2} + rcos\theta)^2} \qquad (1)$$

$$sin\theta_{co}(\theta) = \frac{L_2 n sin\theta}{r_{co}} \qquad (2)$$

Where

$L_1$: distance from (G) center of mass to the big end of the connecting rod.

$L_2$: distance from (G) center of mass to the small end of the connecting rod.

$M_r$: reciprocating mass.

r: crank radius.

λ: ratio of crank shaft radius to connecting rod length.

θ: crank shaft angular displacement.

The connecting rod instantaneous angular displacement and radial distance, given in equations above are periodic functions in terms of the angular displacement(θ) of the crankshaft. Thus in the subsequent analysis, their time derivations producedifficult relationscannotbe manipulated mathematically to acquire the system torsional vibration equations. To obtain differentiable mathematical forms for these expressions, Fourier analysis can be applied [13]. The following system parameters are adopted in order to apply the Fourier analysis, as given in table (1) below.

**Table 1**: Crankshaft-reciprocating parts parameters [4].

| Parameters | Symbol | Value |
|---|---|---|
| **Radius of crankshaft** | r | 75 mm |
| **Mass moment of inertia of crankshaft** | I | 0.03843 kg.m$^2$ |
| **Connecting rod length (from crank end)** | L1 | 111 mm |
| **Connecting rod length** | L | 327 mm |
| **Connecting rod mass** | $M_{co}$ | 6.81 kg |
| **Connecting rod mass moment of inertia** | $I_{cog}$ | 0.032144 kg.m$^2$ |
| **Reciprocating mass** | M | 5.6 kg |

By using the fast Fourier transform (FFT) to $r_{co}$, the following equations are obtained:

$$r_{co}(\theta) = \frac{r_{0co}}{2} + \sum_{n=1}^{\infty} r_{nco}\sin(n\omega t + \phi)$$

$$r_{0co} = \frac{1}{\pi}\int_0^{2\pi} r_{co}(\theta)d\theta$$

$$r_{nco} = \sqrt{a_n^2 + b_n^2}\ ,\ tan\phi = \frac{a_n}{b_n} \qquad (3)$$

$$a_n = \frac{1}{\pi}\int_0^{2\pi} r_{co}(\theta)\cos(n\theta)d\theta$$

$$b_n = \frac{1}{\pi}\int_0^{2\pi} r_{co}(\theta)\sin(n\theta)d\theta$$

By carrying out the numerical integration of the coefficients $r_{0co}$, $a_n$, and $b_n$, the expression of $r_{co}$ can be derived. In the present work, one of the main objectives is to introduce a more rigorous general form for the kinetic energy equation of the system, thus the expression of the radial distance can be expressed in a more general form as:

$$r_{co}(\theta) = D(B + \cos\theta) \quad (4)$$

In the same manner, by applying the Fourier transformation the angular displacement of the connecting rod $\theta_{co}$ may be given by:

$$\theta_{co}(\theta) = A(Fsin\theta + \frac{\sin 2\theta}{2}) (5)$$

Where A, B, D, and F are constants that can be evaluated depending on the system parameters. As a result, in the subsequent analysis, all the necessary equations are derived in terms of these constants. Thus, the substitution results in obtaining system equations in a more general form which subsequently used to analyze the nonlinear torsional vibration of the reciprocating machines by inserting the corresponding system parameters. Consequently, by using the system parameters adopted in the present study (see table (1)), the value of constants A, B, D, and F are (0.25, 1.4907, 0.07508, and 2) respectively.

### *2.2. Torsional Vibration Governing Equations*

The system of a single cylinder internal combustion engine with flywheel is shown in figure (2).

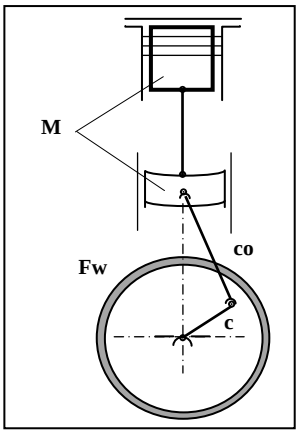


**Figure 2:** Slider-crank mechanism with flywheel of single cylinder ICE [5].
M: reciprocating piston and cross-head shoe; Fw: flywheel; co: connecting rod; c: crank shaft.

By assuming the simple harmonic motion for the reciprocating mass, the system total kinetic energy of a single cylinder slider-crank mechanism may be given by:

$$T = \frac{1}{2} I_{Fw} \dot{\theta}_{Fw}^2 + \frac{1}{2} I \dot{\theta}^2 + E_{co} + \frac{1}{2} M r^2 sin^2\theta \dot{\theta}^2 \quad (6)$$

The connecting rod instantaneous kinetic energy may be expressed inan explicit form by:

$$E_{co} = \frac{1}{2}(I_{cog} + M_{co} r_{co}^2)\dot{\theta}_{co}^2 \quad (7)$$

Where $I_{cog}$represents the connecting rod mass moment of inertia of about the centroid and $M_{co}$represents mass of the connecting rod.
Substituting for expressions of $r_{co}$, and $\theta_{co}$ given in equations (4) and (5), yields the following system kinetic energy in terms of the crankshaft angular displacement θ:

$$T = \frac{1}{2} I_{Fw} \dot{\theta}_{fw}^2 + \frac{1}{2} I \dot{\theta}^2 + \frac{1}{2} M r^2 sin^2\theta \dot{\theta}^2 + \frac{1}{2}\left( I_{cog} + M_{co}(D(B + cos\theta))^2\right)\left(A(Fcos\theta - cos2\theta)\right)^2 \dot{\theta}^2 \quad (8)$$

Also, the system potential energy may be given by:

$$V = \frac{1}{2} k_t (\theta - \theta_{fw})^2 \qquad (9)$$

Where $k_t$ represents the crankshaft torsional stiffness constant.
The system torsional vibration equation of motion can be derived by applying the Lagrange's rule as a function of the corresponding coordinate θ such that:

$$\frac{d}{dt}\left(\frac{\partial T}{\partial \dot{\theta}}\right) - \frac{\partial T}{\partial \theta} + \frac{\partial V}{\partial \theta} = Q_{noncon} \qquad (10)$$

By inserting equations (8) and (9), in equation (10) yields:

$$\begin{bmatrix} \left(I + \frac{Mr^2}{2} + I_{cog}A^2\left(\frac{1+F^2}{2}\right) + M_{co}D^2\left(\left(B^2+\frac{1}{2}\right)\left(\frac{F^2+1}{2}\right) + \frac{F^2}{8} - 8F\right)\right) - \frac{Mr^2}{2}(cos2\theta) + \\ I_{cog}A^2\left(\frac{F^2}{2}cos2\theta + \frac{cos4\theta}{2} - 2Fcos\theta cos2\theta\right) + M_{co}D^2A^2 \begin{pmatrix} \left(2B\left(\frac{F^2+1}{2}\right) - \frac{F}{2}\right)cos\theta + \\ \left(\frac{F^2}{2}\left(B^2+\frac{1}{2}\right) - \right) \\ 2BF + \left(\frac{F^2+1}{4}\right) \end{pmatrix} cos2\theta + \\ \left(\frac{1}{2}\left(B^2+\frac{1}{2}\right) - BF + \frac{F^2}{8}\right)cos4\theta + \\ \left(BF^2 - 2F\left(B^2+\frac{1}{2}\right)\right)cos\theta cos2\theta + \\ \left(\frac{1}{2}\left(B+\frac{1}{2}\right)\right)cos2\theta cos4\theta - \frac{F}{2}cos4\theta \end{pmatrix} \end{bmatrix} \ddot{\theta} +$$

$$\begin{bmatrix} \frac{Mr^2}{2}(sin2\theta) + I_{cog}A^2\left(-\frac{F^2}{2}sin2\theta + 2Fsin\theta cos2\theta + 2Fcos\theta sin2\theta - sin4\theta\right) + \\ M_{co}D^2A^2 \begin{pmatrix} \left(-\frac{1}{2}\left(2B\left(\frac{F^2+1}{2}\right) - \frac{F}{2}\right)sin\theta\right) - \left(\frac{F^2}{2}\left(B^2+\frac{1}{2}\right) - 2BF + \left(\frac{F^2+1}{2}\right)\right)sin2\theta - \\ 2\left(\left(B^2+\frac{1}{2}\right) - BF + \frac{F^2}{8}\right)sin4\theta - \left(\frac{B}{2}+\frac{1}{4}\right)sin2\theta cos4\theta - \\ \left(BF^2 - 2F\left(B^2+\frac{1}{2}\right)\right)sin2\theta cos\theta - \frac{1}{2}\left(BF^2 - 2F\left(B^2+\frac{1}{2}\right)\right)sin\theta cos2\theta - \\ 2\left(\frac{B}{2}+\frac{1}{4}\right)sin4\theta cos2\theta + \frac{F}{4}sin\theta cos4\theta + Fsin4\theta cos\theta \end{pmatrix} \end{bmatrix} \dot{\theta}^2 +$$

$$k_t(\theta - \theta_{fw}) = Q_{noncon} \qquad (11)$$

The equation above represents the general form of the nonlinear torsional vibration of a single cylinder engine tokening into account the variable inertiaeffect of the reciprocating masses and non-conservative forces. At current work, the non-conservative forces represented by the internal damping and gas forces. Thus in the subsequent sections, their effects incorporated with the non-constant inertia effect are explored in detail.

### *2.3. Nonlinear Torsional Vibration Modelling:Free Vibration*

The effect of nonconstant inertia the reciprocating masses in single cylinder can be detected by using equation (11) with assuming the term $Q_{noncon}$ to be equal zero. A non-dimensional conversion can be achieved for equation (11) by introducing the following expressions:

$\alpha = \theta - \theta_{FW}$
$\theta = \omega t + \alpha$
$\tau = \omega t$
$\frac{d(\,)}{dt} = \omega \frac{d(\,)}{dt} = \omega(\,)'$

$$f_r = \frac{\omega^2}{k_t/I_{eq}} = \frac{\omega^2}{{\omega_n}^2}$$

$$I_{eq} = \left(I + \frac{Mr^2}{2} + I_{cog}A^2\frac{\left(1+F^2\right)}{2}\right) + M_{co}D^2A^2\left(\left(B^2+\frac{1}{2}\right)\left(\frac{F^2+1}{2}\right) + \frac{F^2}{8} - BF\right) \qquad (12)$$

$$\varepsilon_1 = \frac{1}{2}\frac{Mr^2}{I_{eq}}$$

$$\varepsilon_2 = \frac{I_{cog}A^2}{I_{eq}}$$

$$\varepsilon_2 = \frac{M_{co}D^2A^2}{I_{eq}}$$

Where:
$f_r$: frequency ratio.
$I_{eq}$: system equivalent mass moment of inertia.
$\alpha$: torsional vibration displacement.
$\omega$:crank shaft angular speed.
$\omega_n$: natural frequency of the system.
$\tau$: dimensionless time.
$\varepsilon_1$, $\varepsilon_2$, $\varepsilon_3$: inertia ratios of reciprocating masses, mass moment of inertia of connecting rod and mass of connecting rod respectively.
By inserting equation (12) in equation (11) and disregarding the product terms, derivative terms, and higher order terms, so that equation (11) yields:

$$\left(1 - \varepsilon_1(cos2\tau) + \varepsilon_2\left(A_1cos2\tau - A_2cos\tau cos2\tau + \frac{1}{2}cos4\tau\right) + \varepsilon_3\begin{pmatrix}A_3cos\tau + A_4cos2\tau + \\ A_7cos2\tau cos4\tau + \\ A_6cos\tau cos2\tau + \\ A_7cos2\tau cos4\tau - \\ A_8cos\tau cos4\tau\end{pmatrix}\right)\alpha'' +$$

$$2\left(\varepsilon_1(-sin2\tau) + \varepsilon_2\begin{pmatrix}A_1sin2\tau - \frac{A_2}{2}sin\tau cos2\tau \\ -A_2sin2\tau cos\tau + sin4\tau\end{pmatrix} + \varepsilon_3\begin{pmatrix}\frac{A_3}{2}sin\tau + A_4sin2\tau + 2A_5sin4\tau + \\ \frac{A_6}{2}sin\tau cos2\tau + A_6sin2\tau cos\tau + \\ A_7sin2\tau cos4\tau + 2A_7sin4\tau cos2\tau \\ -\frac{A_8}{2}sin\tau cos4\tau - 2A_8sin4\tau cos\tau\end{pmatrix}\right)\alpha' +$$

$$\left(\varepsilon_1(-2cos2\tau) + \varepsilon_2\begin{pmatrix}2A_1cos2\tau - \\ 2.5A_2cos\tau cos2\tau + \\ 4cos4\tau\end{pmatrix} + \varepsilon_3\begin{pmatrix}\frac{A_3}{2}cos\tau + 2A_4cos2\tau + \\ 8A_5cos4\tau + 2.5A_6cos\tau cos2\tau + \\ 10A_7cos2\tau cos4\tau - 8.5A_8cos\tau cos4\tau\end{pmatrix} + \frac{1}{f_r^2}\right)\alpha =$$

$$\varepsilon_1(sin2\tau) - \varepsilon_2\begin{pmatrix}A_1sin2\tau - \frac{A_2}{2}sin\tau cos2\tau - \\ A_2sin2\tau cos\tau + sin4\tau\end{pmatrix} - \varepsilon_3\begin{pmatrix}\frac{A_3}{2}sin\tau + A_4sin2\tau + 2A_5sin4\tau + \\ \frac{A_6}{2}sin\tau cos2\tau + A_6sin2\tau cos\tau + \\ A_7sin2\tau cos4\tau + 2A_7sin4\tau cos2\tau - \\ \frac{A_8}{2}sin\tau cos4\tau - 2A_8sin4\tau cos\tau\end{pmatrix} \qquad (13)$$

Where the constants $A_1$ to $A_8$ are given by:

$$A_1 = \frac{F^2}{8}, A_2 = 2F$$

$$A_4 = \frac{F^2}{2}\left(B^2 + \frac{1}{2}\right) - 2BF + \left(\frac{F^2+1}{4}\right)$$

$$A_5 = \frac{1}{2}\left(B^2 + \frac{1}{2}\right) - BF + \frac{F^2}{8}$$

$$A_6 = BF^2 - 2F\left(B^2 + \frac{1}{2}\right)$$

$$A_7 = \frac{1}{2}\left(B + \frac{1}{2}\right)$$

$$A_8 = \frac{F}{2}$$

Equation (13) given above represents the general form of free nonlinear torsional vibration model including all the non-constant inertia terms arises due to the motion of reciprocating parts.

***2.4. Nonlinear Torsional Vibration Modelling: Damped-Forced Vibration***

The interaction between the variable inertia effect, nonlinear damping, and gas forces on nonlinear torsional vibration modeling can be investigated by inserting the mathematical models of nonlinear damping and gas forces in equation (11). A comprehensive model for the internal damping of a single cylinder ICE including all the types of damping due to viscous friction, material hysteresis, and non-friction was presented by [4], and it is adopted in the current analysis. The model of nonlinear damping is given by:

$$Q_{noncon} = -(C_h + C_1 cos2\theta - C_2 sin\theta sin2\theta - C_3 cos4\theta + C_4 cos6\theta + C_5 cos\theta cos3\theta) \quad (14)$$

Where C to $C_5$ are damping constants given by:

$$C_h = 1.5C_c + \left(\frac{1}{2} + \frac{\lambda_2^2}{8}\right)(c_{p1} + c_{p2}) + c_{R1}\left(\frac{\lambda_1^2}{2} + \frac{\lambda_2^2}{2}\right) + c_{R2}\left(\frac{(1+\lambda_1)^2}{2} + \frac{\lambda_2^2}{2}\right)$$

$$C_1 = \frac{C_{R1}\lambda_1^2}{2} + \frac{C_{R2}(1+\lambda_1)^2}{2} - \frac{(C_{P1} + C_{P2})}{2}$$

$$C_2 = \lambda(C_{P1} + C_{P2})$$

$$C_3 = \frac{\lambda_2^2}{8}(C_{P1} + C_{P2})$$

$$C_4 = \frac{\lambda_2^2}{2}(C_{R1} + C_{R2})$$

$$C_5 = 2\left(C_{R1}\lambda_1\lambda_2 + C_{R2}\lambda_2(1+\lambda_1)\right)$$

And

$\lambda = \frac{r}{L_1+L_2}$ , $\lambda_1 = \lambda + \frac{\lambda^3}{8}$, $\lambda_2 = \frac{\lambda^3}{8}$

For the external excitation torque, many researchers have shown that the excitation torque due to gas forces can be given as a function of crankshaft angular displacement (θ)[14-15]:

$$M_g = \frac{\pi D_b^2}{4} P(\theta)\left(sin\theta + \frac{\lambda}{2}\frac{sin2\theta}{\sqrt{1 - \frac{\lambda^2}{2} + cos2\theta}}\right) \quad (15)$$

Where:

$D_b$: cylinder bore dimeter.

P(θ): combustion gas pressure as a function of crank angle (θ).

For simplicity of analysis, the gas pressure is assumed to be of averaged value ($P_{avg}$) to compare its effects on excitation torque. Thus, by substituting equations (14) and (15) in equation (11) with using expressions given in equation (12), and disregarding the product terms, derivative terms, and higher order terms, so that equation (11) yields:

$$\left(\begin{matrix}1-\varepsilon_1(cos2\tau)+\\ \varepsilon_2\left(A_1cos2\tau-A_2cos\tau cos2\tau+\frac{1}{2}cos4\tau\right)+\varepsilon_3\left(\begin{matrix}A_3cos\tau+A_4cos2\tau+\\ A_5cos4\tau+A_6cos\tau cos2\tau+\\ A_7cos2\tau cos4\tau-A_8cos\tau cos4\tau\end{matrix}\right)\end{matrix}\right)\alpha''+$$

$$2\left(\begin{matrix}-\varepsilon_1(sin2\tau)+\varepsilon_2\left(A_1sin2\tau-\frac{A_2}{2}sin\tau cos2\tau-A_2sin2\tau cos\tau+sin4\tau\right)+\\ \varepsilon_3\left(\begin{matrix}\frac{A_3}{2}sin\tau+A_4sin2\tau+2A_5sin4\tau+\frac{A_6}{2}sin\tau cos2\tau+A_6sin2\tau cos\tau+\\ A_7sin2\tau cos4\tau+2A_7sin4\tau cos2\tau-\frac{A_8}{2}sin\tau cos4\tau-2A_8sin4\tau cos\tau\end{matrix}\right)+\\ \frac{\zeta}{f_r}(1+\zeta_1cos2\tau-\zeta_2sin\tau sin2\tau+\zeta_3cos4\tau+\zeta_4cos6\tau+\zeta_5cos\tau cos3\tau)\end{matrix}\right)\alpha'+$$

$$\left(\begin{matrix}-2\varepsilon_1(cos2\tau)+\varepsilon_2(2A_1cos2\tau-2.5A_2cos\tau cos2\tau+4cos4\tau)+\\ \varepsilon_3\left(\begin{matrix}\frac{A_3}{2}cos\tau+2A_4cos2\tau+8A_5cos4\tau+\\ 2.5A_6cos\tau cos2\tau+10A_7cos2\tau cos4\tau-8.5A_8cos\tau cos4\tau\end{matrix}\right)-\\ \frac{2\zeta\zeta_2}{f_r}(sin\tau cos2\tau+sin2\tau cos\tau)-\frac{K_r}{f_r^2}\left(cos\tau+\frac{\lambda cos2\tau}{\sqrt{1-\frac{\lambda^2}{2}+\frac{cos2\tau}{2}}}\right)+\frac{1}{f_r^2}\end{matrix}\right)\alpha=$$

$$\varepsilon_1(sin2\tau)-\varepsilon_2\begin{pmatrix}A_1sin2\tau-\frac{A_2}{2}sin\tau cos2\tau\\ -A_2sin2\tau cos\tau+sin4\tau\end{pmatrix}-\varepsilon_3\left(\begin{matrix}\frac{A_3}{2}sin\tau+A_4sin2\tau+2A_5sin4\tau+\\ \frac{A_6}{2}sin\tau cos2\tau+A_6sin2\tau cos\tau+\\ A_7sin2\tau cos4\tau+2A_7sin4\tau cos2\tau-\\ \frac{A_8}{2}sin\tau cos4\tau-2A_8sin4\tau cos\tau\end{matrix}\right)-$$

$$\frac{2\zeta}{f_r}\begin{pmatrix}1+\zeta_1cos2\tau-\zeta_2sin\tau sin2\tau+\\ \zeta_3cos4\tau+\zeta_4cos6\tau+\zeta_5cos\tau cos3\tau\end{pmatrix}+\frac{K_r}{f_r^2}\qquad(16)$$

Where the damping ratios $\zeta$ to $\zeta_5$ are given by:

$$\zeta=\frac{C}{2\omega_nI_{eq}},\ \zeta_1=\frac{C_1}{C},\ \ \zeta_2=\frac{C_2}{C},\ \zeta_4=\frac{C_4}{C},\ \ \zeta_5=\frac{C_5}{C}$$

Also, the constant $K_g$ and $K_r$ is given by:

$$K_g=\frac{\pi D_b^2}{4}P_{avg}$$

$$K_r=\frac{K_g}{K_t}$$

Equation (16) represents the forced–damped torsional vibration equation of motion of single cylinder ICE taking into consideration the mutual effect of the excitation gas cylinder torque, the effect of internal nonlinear damping and variable inertia of reciprocating parts in a general comprehensive form in terms of the system inertia parameters, damping parameters, and gas force parameters.

## 3. SIMULATION RESULTS

The parametric study can be achieved to examine effects of different system parameters on the dynamic characteristics of the nonlinear torsional vibration of single cylinder internal combustion engine for the three cases of free vibration, damped-free vibration, and damped-forced vibration.

### *3.1. Free-Damped Vibration Results*

A numerical solution for the dynamic model presented by equation (13) has been developed by using Matlab/Simulink. The simulation results show the variations in the effective inertia of the engine sliding and connecting rod parts and the variation in the first mode natural frequency in figures (3) and (4) respectively. The cyclic fluctuations of the engine's effective

mass moment of inertia in each crankshaftangular motion give rise to a periodical variation of frequencies and their corresponding amplitudes, which in turn results in widening the critical speeds range of the engine and induces the phenomenon of secondary excitation rolling torque.

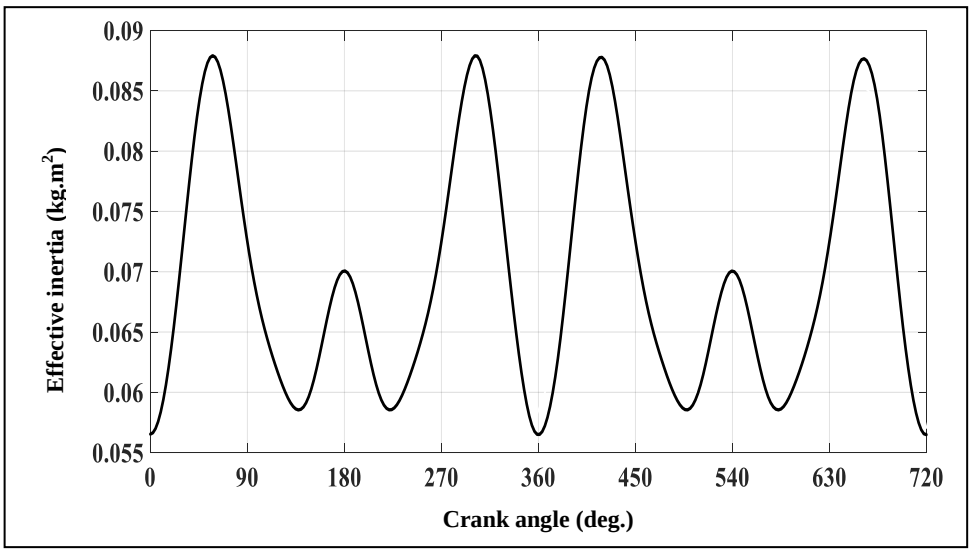


**Figure 3:** Variation in the effective inertia of the system versus crank angle at $f_r = 0.32$.

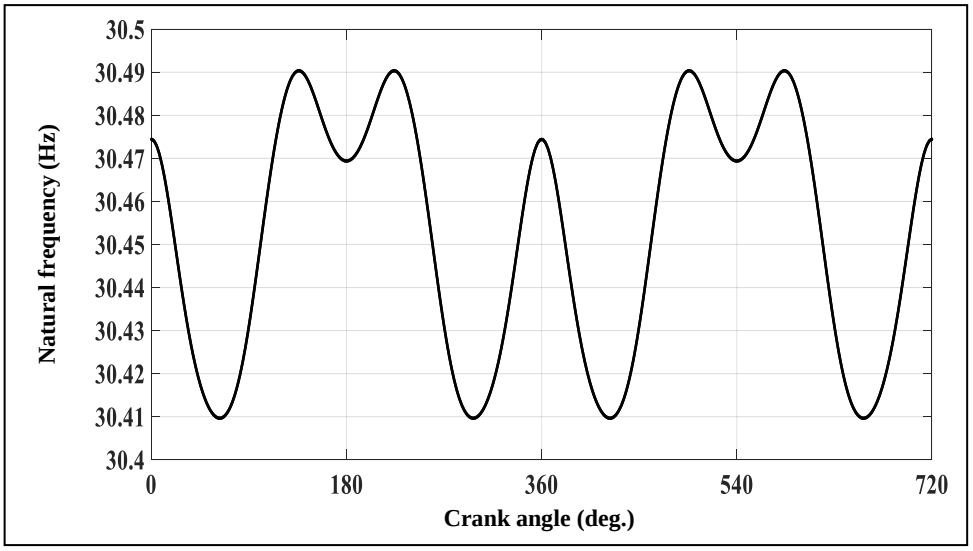


**Figure 4:** Variation in the natural frequency of the system versus crank angle at $f_r = 0.32$.

Also, the results indicated that the consideration of the non-constant inertia in the dynamical analysis leads to improving modeling predictions accuracies for torsional vibration of both single cylinder and multi cylinder engines and can enhance the theory of nonlinear dynamics of reciprocating machines [10].

The variation in the response of the nonlinear torsional vibration displacements at different frequency ratios are shown in figures (5), (6), and (7) respectively. The results displayed that the cyclic variation in the natural frequency of the system produces an unsteady torsional amplitude response with obviously dominant beating oscillations, and the response changed to

sustained oscillations of different amplitude and harmonic frequency with increases in the engine speeds. Also, a strong coupling between the torsional angular displacement response and the engine speed is revealed, which show that the critical range of the engine speed is increased and widened in their zones.

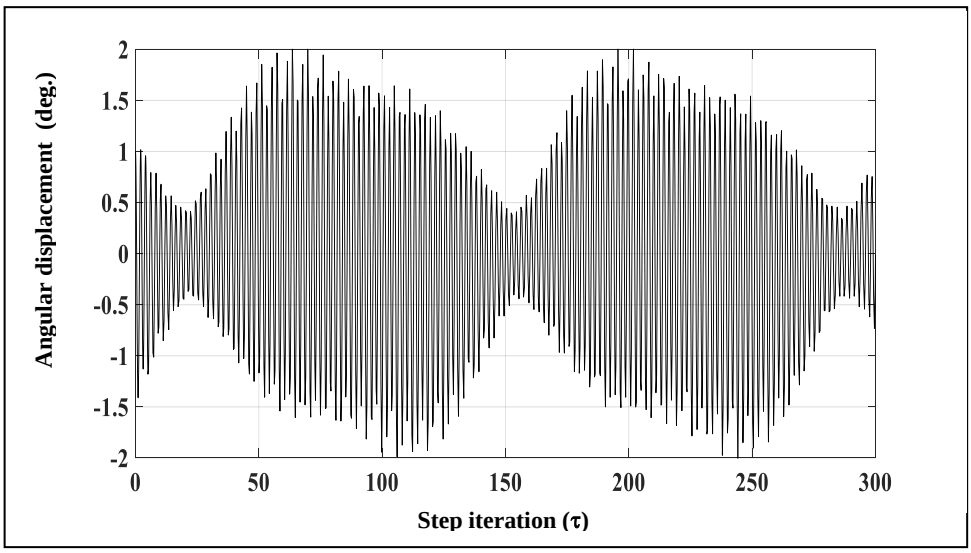


**Figure 5:** Angular displacement amplitude versus (τ)at fr = 0.33.

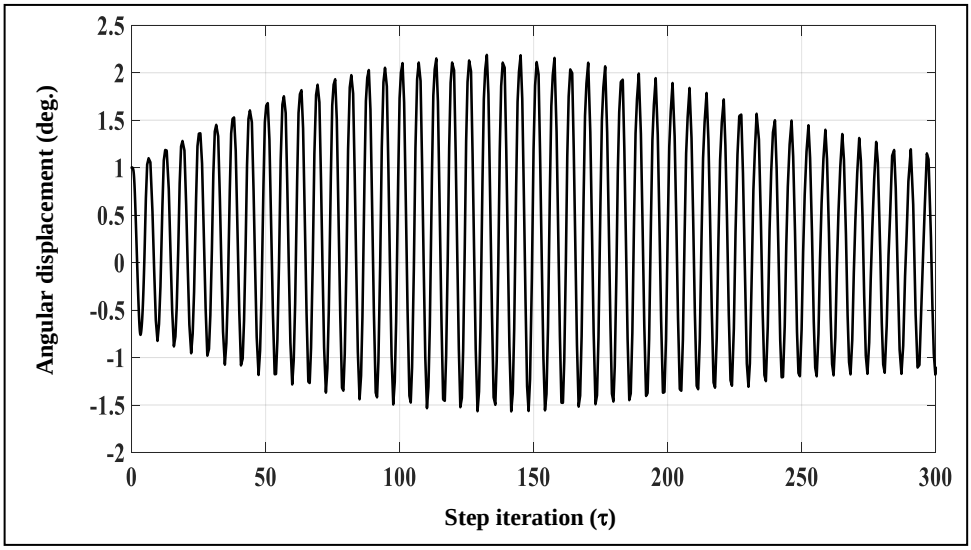


**Figure 6:** Angular displacement amplitude versus (τ) at $f_r$ = 0.99.

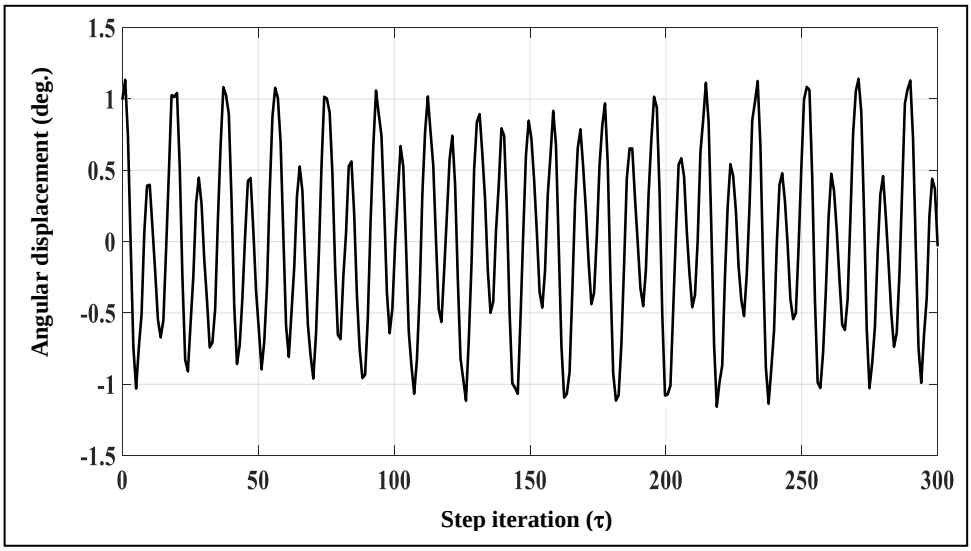


**Figure 7:** Angular displacement amplitude versus (τ) at $f_r = 1.32$.

The variation in the secondary harmonic excitation torque is shown in figure (8), which is indicated that the non-constant inertia consideration leads to arise of the self-excitation secondary excitation torque which in turn results in enhancement of the effective excitation external torque load and produces a range of critical speeds.

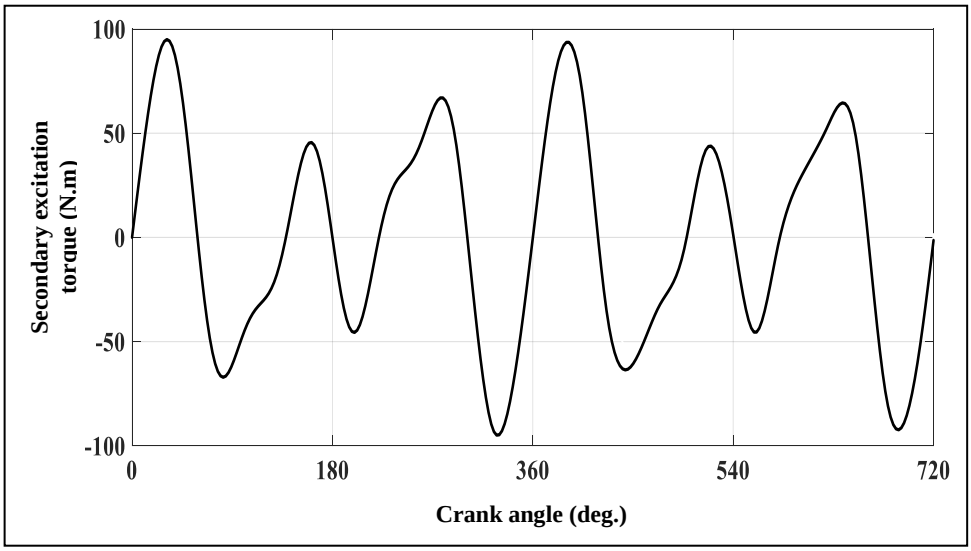


**Figure 8:** Secondary excitation torque versus crank angle at $f_r = 0.33$.

In the same sense the excitation inertia torque amplitude increases dramatically with increasing in the frequency ratio (speed of engine), as depicted in figure (9) and this attributed to the fact that the inertia torque proportional directly with squareof the speed of the engine. Consequently, the additional increase in the inertia torque caused by the non-constant inertia terms enforces the influence of the inertial torque, which produces irregular variation of the angular torsional vibration displacement.

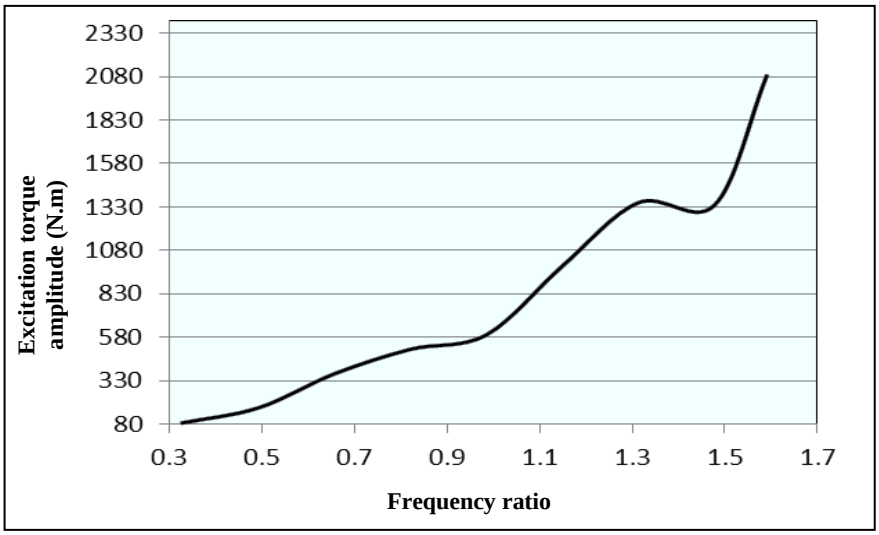


**Figure 9**: Inertia excitation torque amplitude versusfrequency ratio ($f_r$).

The effect of frequency ratio (engine speed) on the free undamped torsional vibration amplitude over a range of harmonic motion (crank angles) is shown in figure (10). The figure depicted that increasesof the speed of the engine produces an increase in the amplitude of vibration and phenomena accompanying them especially with the absence of the damping effect; produces relatively large amplitude induces dangerous vibration stresses leads to a vital failure of the crank assembly.

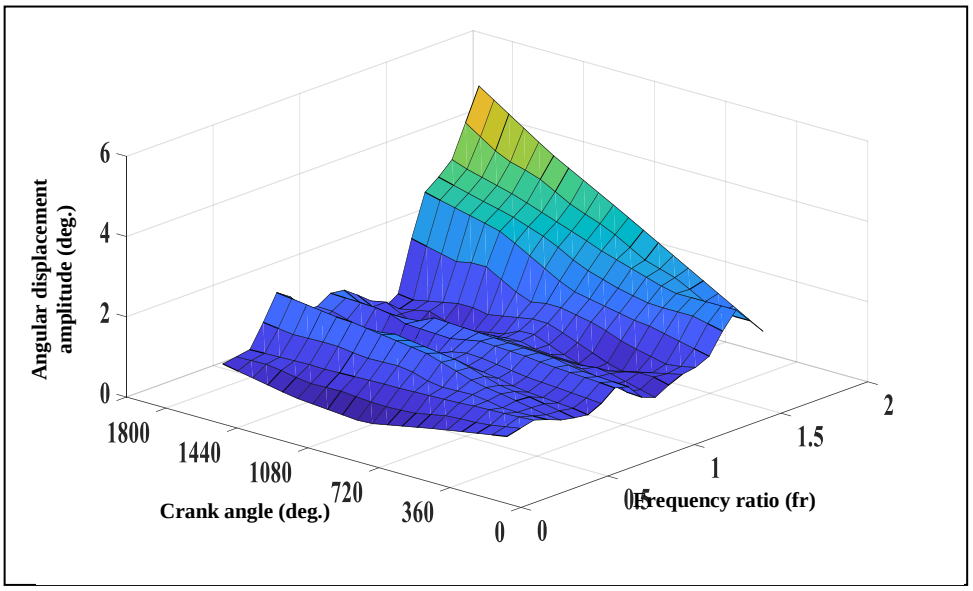


**Figure 10**: Maximum angular displacement amplitude versus crank angle at different frequency ratios.

The results of free-damped vibration can be presented by inserting the damping parameters of the present model in equation (15) and equating the external excitation torque (gas torque) to zero. Table (2) shows the damping parameters adopted in the present study to evaluate their effects on the nonlinear vibration analysis of the internal combustion engine considering the variable inertia of the reciprocating parts.

**Table 2**: Crank, connecting rod, and slider damping parameters [4].

| Parameters | Symbol | Value$\left(\frac{N.m}{rad/sec}\right)$ |
|---|---|---|
| **Crankshaft total damping** | $C_c$ | 0.5828 |
| **Slider head damping** | $C_{P1}$ | 0.09 |
| **Cross-head damping** | $C_{P2}$ | 0.0549 |
| **Connecting rod upper joint damping** | $C_{R1}$ | 0.2864 |
| **Connecting rod lower joint damping** | $C_{R2}$ | 0.3024 |

One of the critical concerns in the torsional vibration of ICE is the inherent torsional resonances and corresponding amplitudes ranges of the crankshaft assembly, and the ability to quantify these natural modes more precisely requires a better understanding of the damping characteristics [4, 11]. The variation of the effective damping of the crankshaft assembly over a crankshaft angular displacement is presented in figure (11). It can be seen that the cyclic variation of the damping shows clearly the nonlinear inherent characteristics of the engine damping, which in turn leads to modified system frequencies and amplitudes variation over crank cycles, as shown in figure (12).

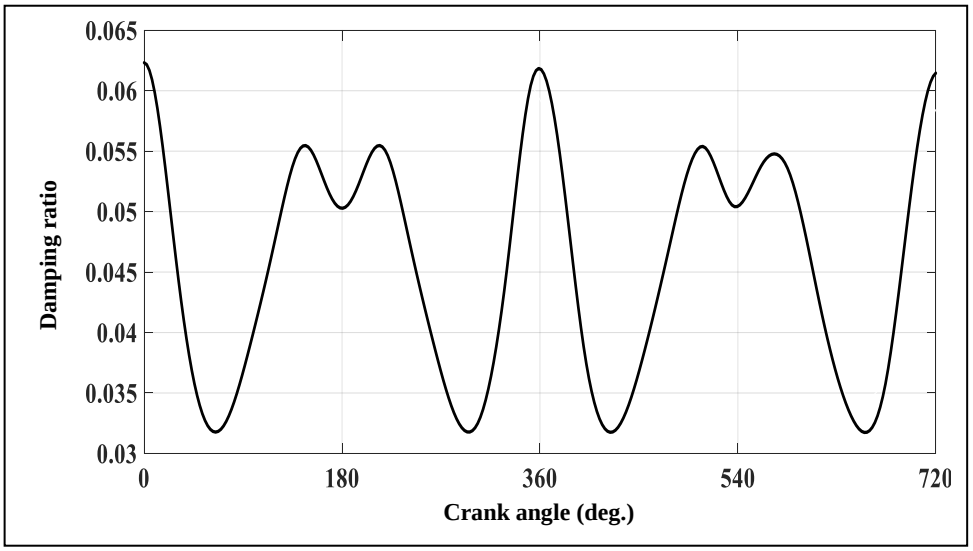


**Figure 11**: Variation of the damping ratio versus crank angle.

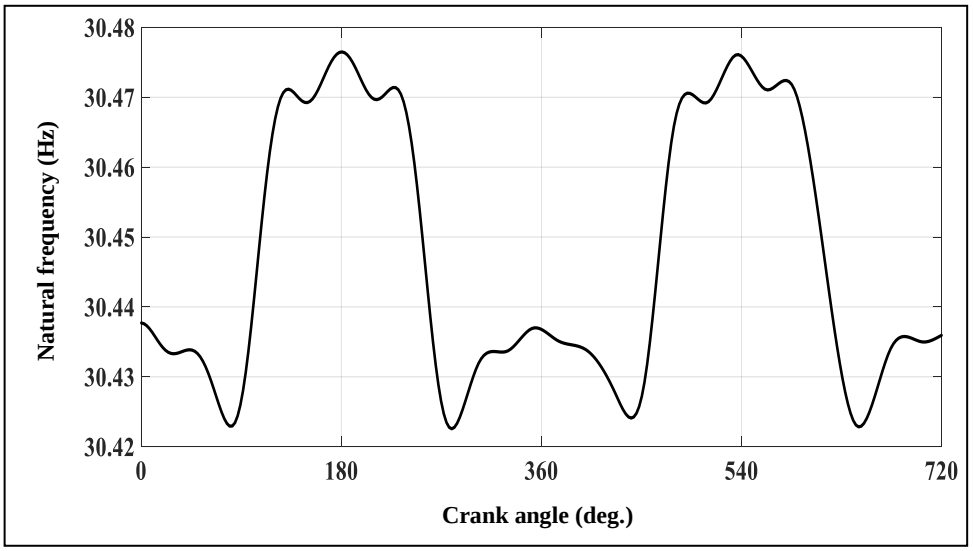


**Figure 12**: Damped frequency of the system versus crank angle.

Alternatively, the damping inherently leads to a change in both the amplitude of frequencies and the harmonic response of the torsional vibration angular displacement and in general causes a decrease in the angular displacement amplitudes of the system, as shown in figures (13), (14), and (15), at different frequency ratios of 0.33, 0.99, and 1.32 respectively. Also, the effect of introducing the nonlinear damping is clearly to be seen for the irregular response of the torsional vibration displacement occurred due to the widening and changing the range of the critical speed of the engine especially at frequencies near the resonance one ($f_r$ =0.33 and 1.32) which appear as a results after taking into account the effect of variation in the inertia of the reciprocating parts in the dynamical analysis.

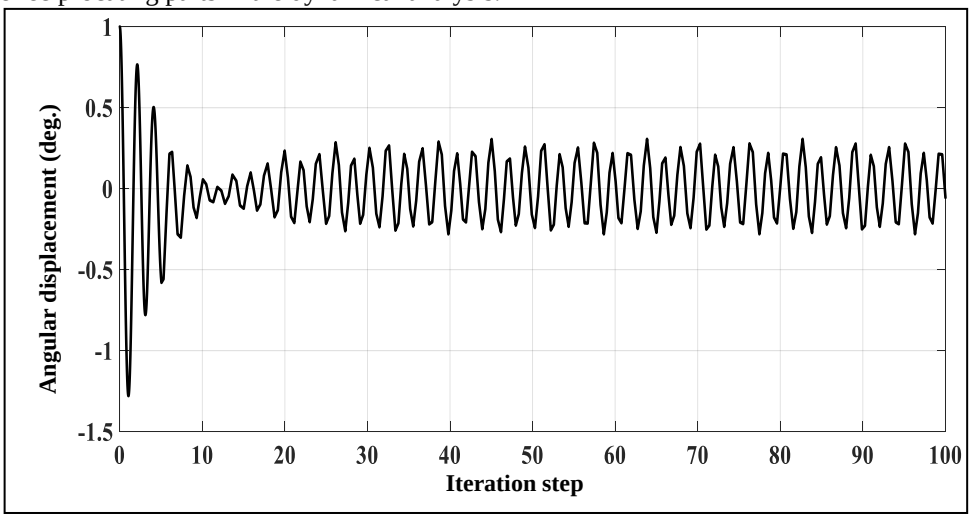


**Figure 13:**Damped angular displacement response versus (τ) at $f_r$ = 0.33.

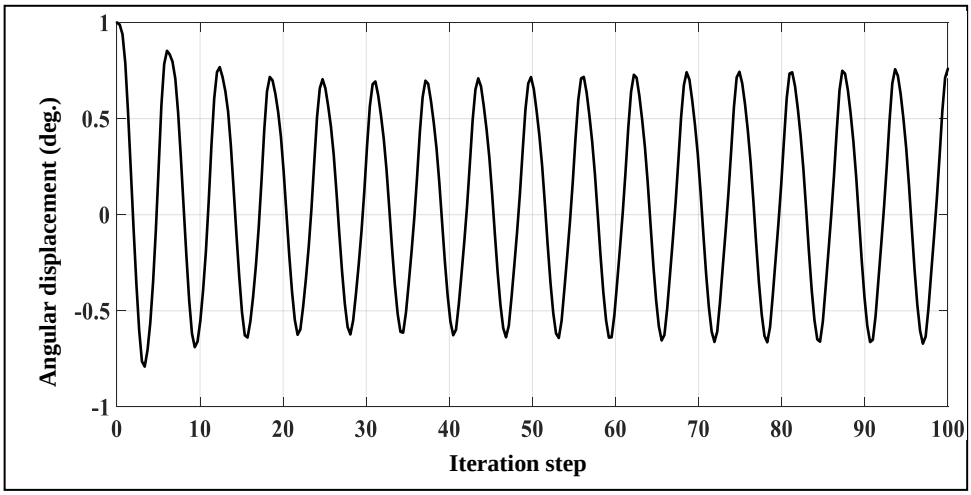


**Figure 14:**Damped angular displacement response versus (τ) at $f_r$ = 0.99.

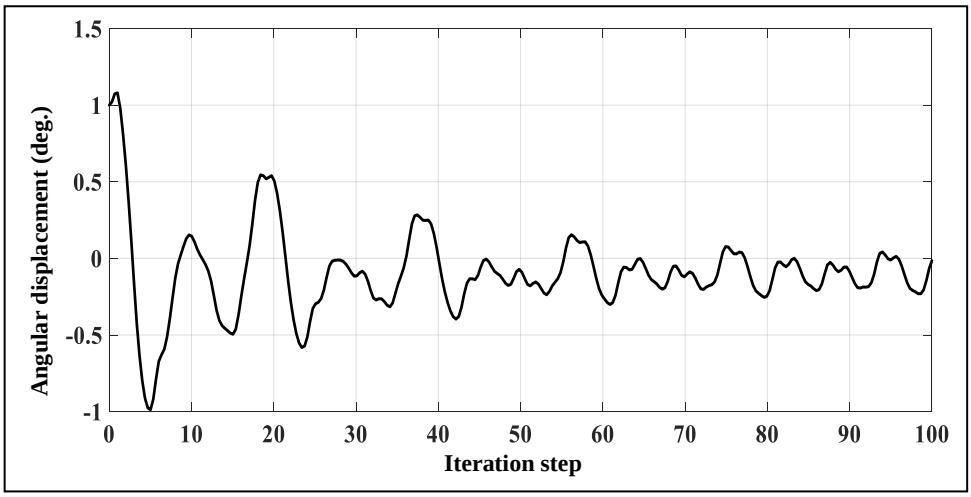


**Figure 15:**Damped angular displacement response versus (τ) at $f_r$ = 1.32.

From point of view of the effect of the nonlinear damping on the excitation torque, the damping torque components with the damping torque arise due to variation in the inertia of the system contributes to an effective reduction in the amplitude of the secondary excitation inertia torque, as shown in figure (16). Consequently, this reduction in the torque amplitude leads to an acceptable reduction in the amplitude of the torsional vibrationdisplacement of the system, as shown in figure (17).

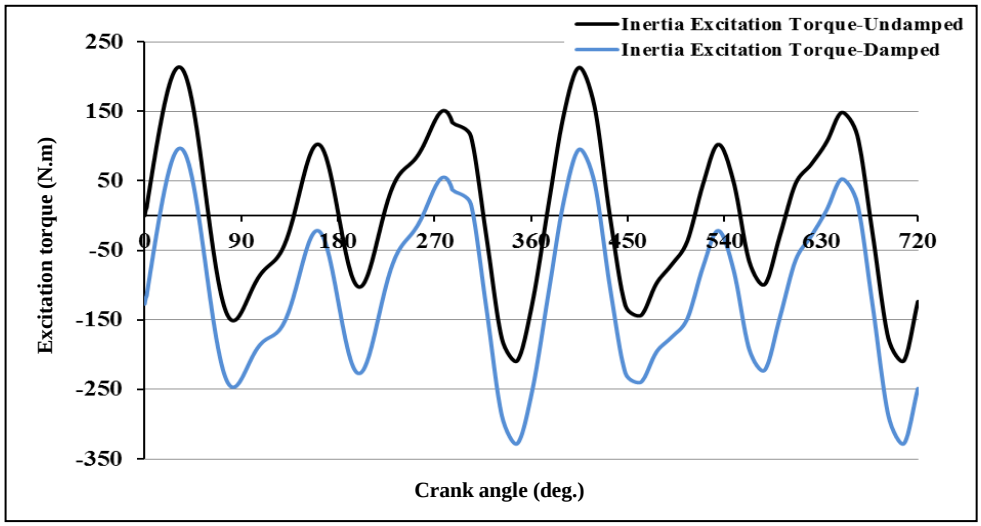


**Figure 16:**Secondary harmonic excitation torque versus crankangle at $f_r$ = 0.49.

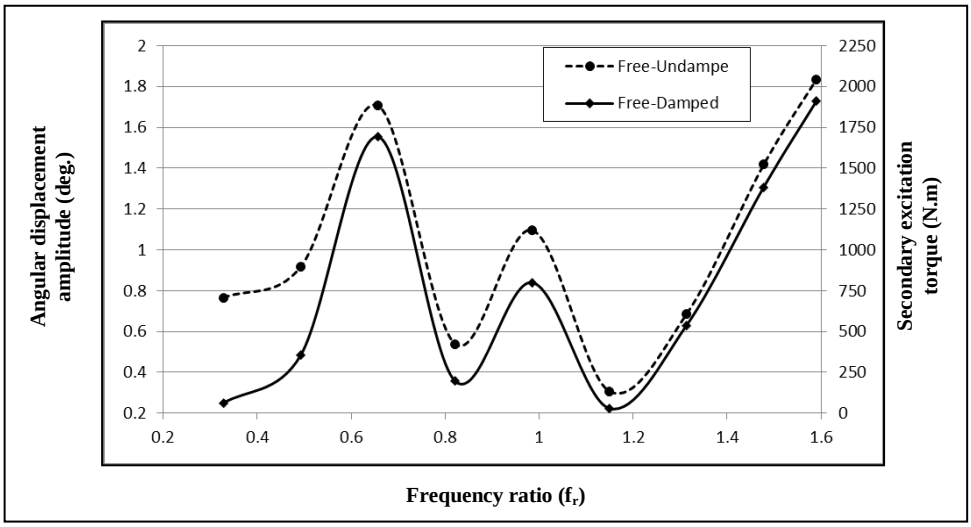


**Figure 17:**Free angular displacement amplitude versus frequency ratio ($f_r$) and secondary excitation torque.

Also with taking into account the variation in the effective inertia of the engine reciprocating masses, shows an increase in the range of the speed over which the system experiences resonance effects which in turn produces resonance amplitudes of relatively large magnitude. Thus, at frequency ratios around the resonance frequency, the amplitude depicted peak values over arrange of frequency ratios. For example, at frequency ratios of 0.67 and 1.59, the amplitude increased around 155.75% and 167.4% compared with that resonance one for the undamped case. While for the damped one, these amplitudes show 141.8 % and 157.7 % increases in their magnitudes at the aforementioned frequencies. Consequently, this shows a reduction of 13.95 % at low frequency ratio and 9.7 % at moderate frequency ratio in the torsional vibration amplitude. These results emphasis on the fact that the variation in the inertia of the crank assembly leads to critical change in the characteristics vibration of the internal combustion engine especially for resonance frequencies and amplitudes. Thus, the validation of theoretical analysis supposed that the major parameter to be verified is the damping [4, 15].

### *3.2. Forced-Damped Vibration Results*

The forced vibration analysis can be carried out by imposing an expression for the external excitation torque gas, as given in equation (15). In the present study, for simulation results purposes, the gas torque is expressed in terms of the $K_r$ factor to explore its mutual effect with secondary inertia excitation torque on the analysis of the torsional vibration of non-constant inertia of a single-cylinder ICE. In general, when the gas torque acts simultaneously with secondary excitation torque, their amplitudes are strengthened over a crank cycles, as shown in figure (18).

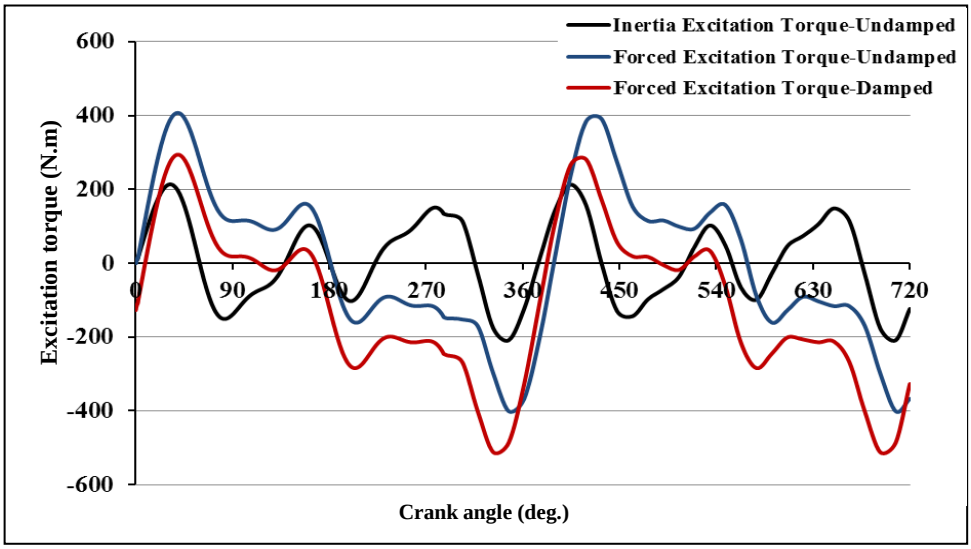


**Figure 18:**Forced excitation torque versus crank angle at fr = 0.49 and Kr = 0.1.

The results also show that the damping effectively reduces the amplitude of the excitation torque compared with the undamped one.

In the same sense, the torsional displacement response is greatly affected by the increase in the amplitude of the excitation torques (gas torque and inertia torque), and due to this, the torsional displacement amplitudes and harmonics are depicted large values compared with their values for the free vibration (no damping) case under the same secondary excitation torque, as shown in figure (19).

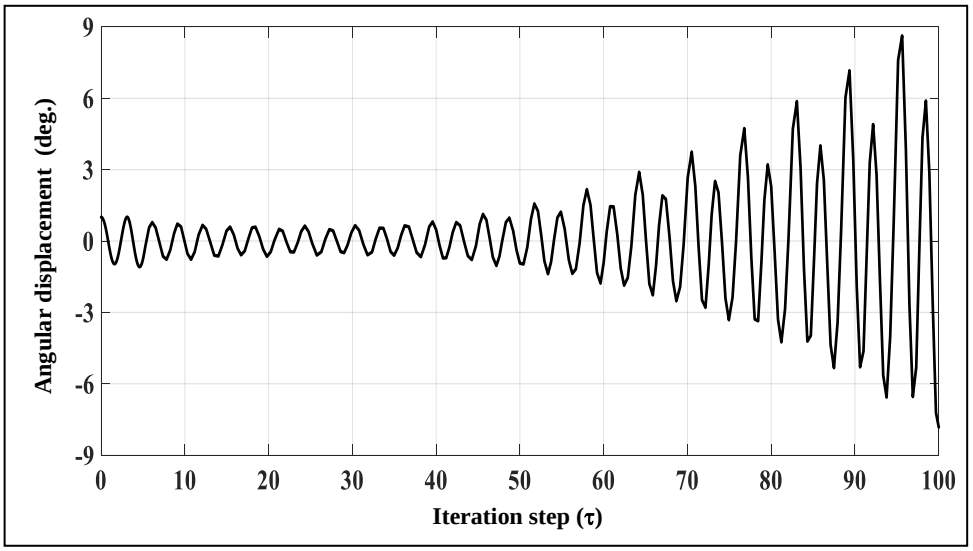


**Figure19:**Forced-damped angular displacement response versus (τ) at $f_r = 0.49$ and $K_r = 0.1$.

Consequently, these variations in the response of the torsional displacement of the crank assembly lead to producing hazardous vibration stress, which in turn may cause the vital failure of the engine assembly. As a result, it is essential to provide the system with effective damping properties to enhance the operational reliability and durability of the internal combustion engine through the full range of engine speeds [1].

## 4. CONCLUSION

1) The present modeling based on the developed expression of the instantaneous kinetic energy of the reciprocating parts provided more enhancements for the knowledge of the effect of the secondary inertia phenomenon when the non-constant inertia terms included in comparison with equivalent or lumped mass models.
2)-Including of non-constant inertia in dynamic modeling produces the inertia excitation torque, damping torque, and additional stiffness.
3)-The inertia excitation torque activates the secondary rolling vibration phenomenon, which results in widening the critical range of the engine speed and altering the resonance amplitudes of the crank assembly of the internal combustion engine.
4) Introducing of nonlinear damping model provides more details for the response of the torsional vibration displacement amplitude and harmonic frequencies, and variation in natural frequency of the crank – reciprocating assembly.
5) The nonlinear damping introduces a reduction in the amplitude of the torsional vibration displacement of 3.95 % at low-frequency ratio(engine speed) and 9.7 % at moderate frequency ratio (engine speed).
6) The damped free vibration results show that the amplitude of the damped inertia excitation torque is less than that of the undamped inertia excitation torque.
7) The forced vibration results show that the external excitation torque amplitudes are strengthened by the inertia excitation torque and can produce hazardous vibration amplitudes and stress, and in the spite of this, the damping work well to decrease the amplitude of the torsional vibration displacement.

## REFERENCE


[1] W. Homik, A. Mazurkow, and P. Woś, "Application of a Thermo-Hydrodynamic Model of a Viscous." Multidisciplinary Digital Publishing Institute (MDPI). [Online]. Available: https://www.ncbi.nlm.nih.gov/pmc/articles/PMC8469732/ [Accessed: Feb. 14, 2022].

[2] A. L. Guzzomi, D. C. Hesterman, and B. J. Stone, "Variable inertia effects of an engine including piston friction and a crank or gudgeon pin offset." Journal of Automobile Engineering, vol. 222, no. 3, pp. 397-414, 2008.

[3] J. Pankiewicz and M. Zawisza, "Research of torsional vibration of the internal combustion engine's crankshaft with various dampers (TVD)." VIBROENGINEERING PROCEDIA. vol. 3, pp. 229-232 2014.

[4] Y. WANG and T. LIM, "Effects of Viscous Friction and Non- Friction Damping Mechanism inaReciprocating engine." Journal of Sound and Vibration, vol. 257, no. 1, pp. 177-188, 2002.

[5] B. Hector, E. Carlos, Ugalde-Loo, and A. Muditha, "Dynamic Modelling and Control of a Reciprocating Engine," 9 the International Conference on Applied Energy, pp.1282–1287, 2017.

[6] A. Enrico, C. Francesco, E. Luca, G. Venanzio and C. Roberto, "Multibody Simulation for the Vibration Analysis of a Turbocharged Diesel Engine," Appl. Sci. 8, 1192. 2018. [Online]. Available: https://www.researchgate.net/publication/326554249. [Accessed: Nov. 29, 2021].

[7] N. K. JOSHI and V. K. PRAVIN, "Analysis of the Impact of Variable and Non-variable Inertia on Torsional Vibration Characteristics of marine Propulsion Plant Driven by Diesel Engine," International Journal of Mechanical and Production Engineering Research and Development, Vol. 4, Issue 1, pp.113-124, Feb 2014.

[8] N. K. JOSHI and V. K. PRAVIN, "Analysis of the Impact of Variable and Non-variable Inertia on Torsional Vibration Characteristics of marine Propulsion Plant Driven by Diesel Engine," International Journal of Mechanical and Production Engineering Research and Development, Vol. 4, Issue 1, pp.113-124, Feb 2014.

[9] F. Jabbar, G. Hassan, A. Karim, akilabadi, K. Hadi, " the Effect of Damping Coefficient on the Torsional Vibration of the Damped Multi-branch Gears System," Journal of Applied Mathematics and Computational Mechanics, 16 (4), pp.5-16, 2017.

[10] M. Pasricha, "Effect of Damping on Parametrically Excited Torsional Vibrations of Reciprocating Engines Including Gas Forces," Journal of Ship Research, Vol. 50, No. 2, June, pp. 147-157, 2006.

[11] V. Nenad, Đ. Dobrota, and I. Komar, "Damping and Excitation in the Torsional Vibrations Calculation of Ship Propulsion Systems," International Scientific and Professional Conference Contemporary issues in economy and technology (CIET), pp. S-165-S-174, 2018.

[12] T. Li, Z. Huang, C. Zhen, Z. Kehai, W. Jie, "Analysis of the Influence of Piston-Cylinder Friction on the Torsional Vibration Characteristics of Compressor Crankshaft System, " Pre Print on Research Square, March 2022. [Online]. Available: https://www.researchsquare.com/article/rs-1464003/latest.pdf (accessed: Aug. 27, 2022).

[13] S.S. Rao, Mechanical Vibrations, 5th edition, Pearson Education, Inc. 2011.

[14] C. LONG, S. WENKU, and C. ZHIYONG, "Research on Damping Performance of Dual Mass Flywheel Based on Vehicle Transmission System Modeling and Multi-Condition Simulation," IEEE Access. https://ieeexplore.ieee.org/document/8998315. [Accessed: July 13, 2022].

[15] S. Hasmet, T. Mustafa, "Optimization of Torsional Vibration Damper of Cranktrain System Using a Hybrid Damping Approach," Engineering Science and Technology, an International Journal, 24, pp. 959–973, 2021.